μ-Metal Wire Magnetic Shields for Large PMTs

Vahe Ghazikhanian
Department of Physics, UCLA, Los Angeles, CA 90095
Kirk T. McDonald
Joseph Henry Laboratories, Princeton University, Princeton, NJ 08544

(February 24, 2007)

This note draws attention to the technique of the ANTARES Collaboration to shield large PMTs in a spherical mesh of μ-metal wire. Such a shield improves the single-photoelectron peak-to-valley ratio by 50% and renders the PMT gain essentially independent of orientation.

The effect of the Earth's magnetic field, whose typical strength is 0.3-0.5 gauss, on the performance of a photomultiplier tube (PMT) is twofold:

- The trajectories of photoelectrons are affected such that the collection efficiency at the first dynode is a function of the orientation of the PMT relative to the magnetic field.

  For example, an unshielded 8″ Hamamatsu R5912 PMT showed ±6% gain variation as a function of orientation relative to the Earth's magnetic field in tests conducted by the Auger Collaboration [1, 2, 3], shown on the left below.

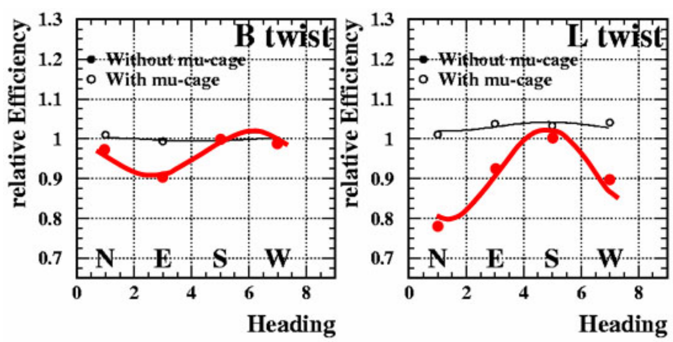

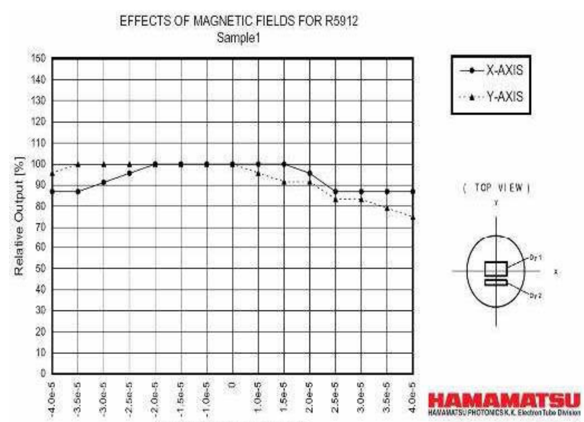

  Note that the gain of a well-designed PMT such as the Hamamatsu R5912 is largely unaffected by magnetic fields large than $\approx 1/3$ of the Earth's field, as shown in the figure on the right above.

- The trajectories of secondary electrons in the dynode chain are affected such as to increase fluctuations in the PMT gain. This causes a lower "peak to valley" ratio for single photoelectrons, and increases the average transit time for the signal.

  For example, an unshielded 10″ Hamamatsu R7081 PMT showed a 30% lower peak-to-valley ratio and a 1-ns long transit time for single photoelectrons compared to a shielded PMT, in studies by the ANTARES Collaboration [4, 5, 6].

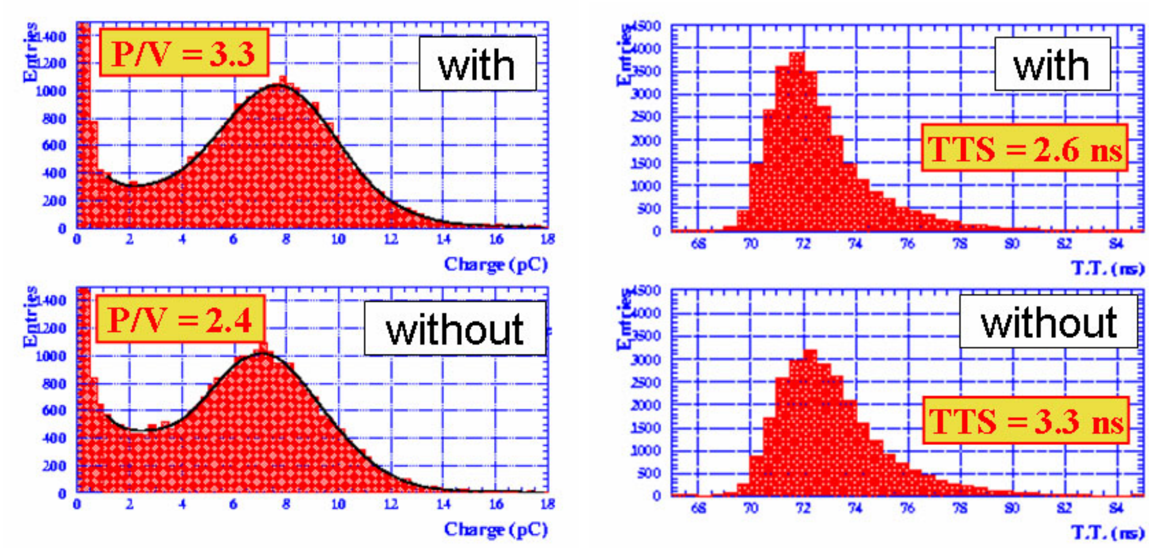

These effects are not large, so that many experiments, including LSND [7], and mini-BooNE [8] and the Pierre Auger Project [9], operate large PMTs with no magnetic shielding (since the classic technique of shielding a PMT with a μ-metal cylinder is awkward for large PMTs in tanks of liquids). Other experiments, including Super-Kamiokande [10], SNO [11], KamLAND [12] and BOREXINO [13], surround the entire detector with field-compensating coils to cancel some components of the Earth's field.

This note draws attention to a variant of the classic μ-metal shield that is well suited to large PMTs in liquid tanks, as pioneered by the DUMAND Collaboration [14] and also used in the NESTOR [15] and ANTARES [4, 5, 6] experiments. Namely, a quasispherical cage of $\approx$ 1-mm diameter wire, whose permeability is $\mu \approx 10^5$, encloses the PMT so as to block only $\approx 8\%$ of the incident light (NESTOR), or $\approx 4\%$ (ANTARES) as shown in the figure below (from [4]).

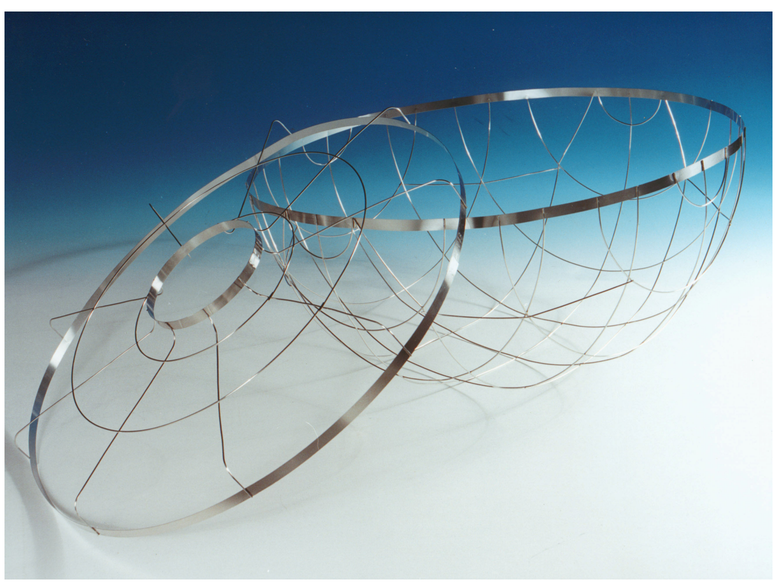

The ANTARES shield reduces the magnetic field strength on the PMT by a factor of ≈ 3 (and ≈ 8 for the NESTOR shield), with the resulting improvement in the single-photoelectron peak-to-valley ratio and transit time as shown in the figures at the top of the page. The variation of PMT gain with orientation is almost completely eliminated, as shown in the figure below (from [4]).

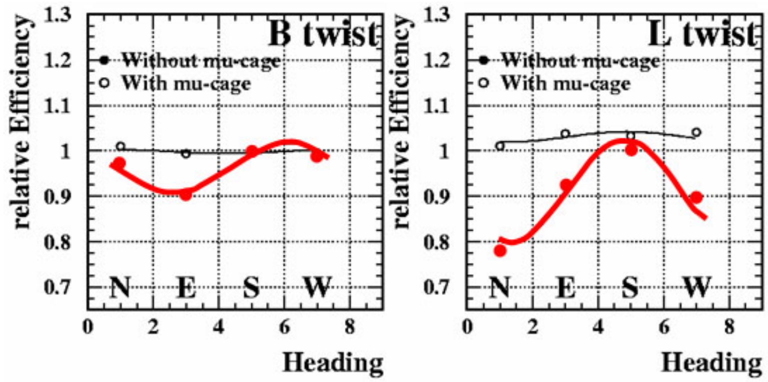

The suppression of the magnetic field by the wire-mesh shield is not fully effective at radii within about one mesh spacing of the mesh itself, and indicated in the figure below (from [16]).

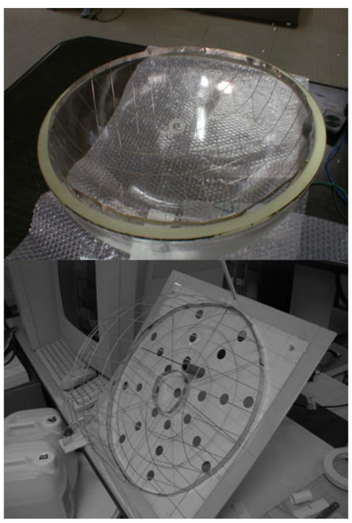

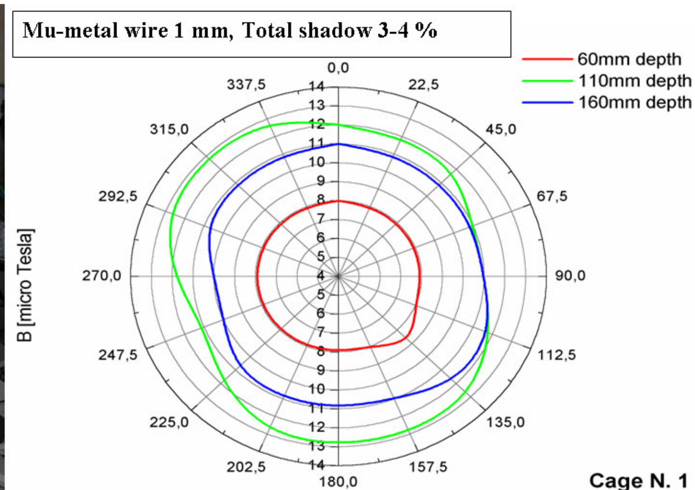

In the Appendix we deduce that a solid shell of high permeability μ, radius a and thickness $\delta a \ll a$ provides a shielding factor of,

$$\frac{H_0}{H_{in}} \approx 1 + \frac{2\mu}{3}\frac{\delta a}{a}\,, \tag{1}$$

where H_0 is the (uniform) external magnetic field and H_{in} is the (uniform) field inside the shell. If the shell is replaced by a wire mesh of thickness δa such that the effective area of the mesh shell is fraction f of a solid shell of radius a, then the shielding factor is roughly,

$$\frac{H_0}{H_{in}} \approx 1 + \frac{2\mu}{3}\frac{\delta a\, f}{a}\,. \tag{2}$$

For example, the ANTARES mesh has $\mu \approx 10^5$, $a = 150$ mm, $\delta a = 1$ mm and $f = 0.04$, for which eq. (2) predicts that $H_0/H_{in} = 2.78$, in good agreement with the observed result.

Appendix: Permeable Shell in a Uniform External Field

We consider a spherical shell of inner radius a and outer radius b made of a material of relative permeability μ that is immersed in an otherwise uniform external magnetic field $\mathbf{B}_0 = \mathbf{H}_0 = -H_0\hat{\mathbf{z}}$, where we use Gaussian units. The magnetic field $\mathbf{H}$ can be deduced from a scalar potential Φ according to $\mathbf{H} = -\boldsymbol{\nabla}\Phi$. The scalar potential corresponding to the external field is,

$$\Phi_0 = H_0 r\cos\theta = B_0 r P_1, \tag{3}$$

in a spherical coordinate system (r, θ, ϕ) whose origin is at the center of the permeable sphere. The potential of the perturbed field will contain only angular functions $P_1(\cos\theta)$, and can be written as,

$$\Phi = \begin{cases} ArP_1 & (r < a), \\ BrP_1 + CP_1/r^2 & (a < r < b), \\ H_0 rP_1 + DP_1/r^2 & (r > b). \end{cases} \tag{4}$$

The magnetic field for $r < a$ is $H_{in} = A$, so we wish to relate this quantity to the external field H_0.

Continuity of the potential at $r = a$ and b requires that,

$$A = B + C/a^3, \tag{5}$$

$$B + C/b^3 = H_0 + D/b^3. \tag{6}$$

The Maxwell equation $\boldsymbol{\nabla}\cdot\mathbf{B} = 0$ implies that the radial component of the magnetic field $\mathbf{B} = \mu\mathbf{H}$ is continuous at the boundaries at $r = a$ and b, and hence,

$$A = \mu(B - 2C/a^3), \tag{7}$$

$$\mu(B - 2C/b^3) = H_0 - 2D/b^3. \tag{8}$$

From eqs. (5) and (7) we find, writing $A = H_{in}$,

$$B = \frac{2\mu+1}{3\mu}H_{in}, \tag{9}$$

and then,

$$C = \frac{\mu-1}{3\mu}a^3 H_{in}. \tag{10}$$

Equation (6) now gives,

$$D = \left[\frac{2\mu+1}{3\mu}b^3 + \frac{\mu-1}{3\mu}a^3\right]H_{in} - b^3 H_0. \tag{11}$$

Inserting eqs. (9)-(11) into eq. (8) we have,

$$\begin{aligned} 3H_0 &= H_{in}\left[\mu\left(\frac{2\mu+1}{3\mu} - 2\frac{\mu-1}{3\mu}\frac{a^3}{b^3}\right) + 2\frac{2\mu+1}{3\mu} + 2\frac{\mu-1}{3\mu}\frac{a^3}{b^3}\right] \\ &= \frac{H_{in}}{3}\left[5 + 4\frac{a^3}{b^3} + 2\left(\mu + \frac{1}{\mu}\right)\frac{b^3 - a^3}{b^3}\right]. \end{aligned} \tag{12}$$

As expected, this form implies that $H_{in} = H_0$ when either $\mu = 1$ or $a = b$.

For a thin, high-permeability shell with $b = a + \delta a$ and $\mu \gg 1$, eq. (12) becomes,[1]

$$\frac{H_0}{H_{in}} \approx 1 + \frac{2\mu}{3}\frac{\delta a}{a}\,. \tag{13}$$

References

[1] P. Ranin *et al.*, *Study of the Influence of the Earth's Magnetic Field on PMTs for Pierre-Auger Surface Detectors* UCLA-Cosmic/2001-02 (May 3, 2001), http://kirkmcd.princeton.edu/examples/detectors/ranin_ucla_cosmic-2001-02.pdf

[2] A.K. Tripathi *et al.*, *Effect of Earth's Magnetic Field on Production Photonis PMTs* UCLA-Cosmic/2001-04 (Dec. 1, 2001), http://kirkmcd.princeton.edu/examples/detectors/tripathi_ucla-cosmic-2001-04.pdf

[3] A.K. Tripathi *et al.*, *A systematic study of large PMTs for the Pierre Auger Observatory*, Nucl. Instr. and Meth. A **497**, 331 (2003), http://kirkmcd.princeton.edu/examples/detectors/tripathi_nim_a497_331_03.pdf
Nucl. Instr. and Meth. A **504**, 1 (2003), http://kirkmcd.princeton.edu/examples/detectors/tripathi_nim_a504_1_03.pdf

[4] P. Vernin and J.-P. Schuller, *The Eyes of ANTARES* (Mar. 8, 2002), http://kirkmcd.princeton.edu/examples/detectors/schuller_antares_030802.ppt

[5] P. Amram *et al.*, *The ANTARES Optical Module*, Nucl. Instr. and Meth. A **484**, 369 (2002), http://kirkmcd.princeton.edu/examples/detectors/amram_nim_a484_369_02.pdf

[6] J.A. Aguilar *et al.*, *Study of large hemispherical photomultiplier tubes for the ANTARES neutrino telescope*, Nucl. Instr. and Meth. A **555**, 132 (2005), http://kirkmcd.princeton.edu/examples/detectors/aguilar_nim_a555_132_05.pdf

[7] C. Athanassopoulos *et al.*, *The liquid scintillator neutrino detector and LAMPF neutrino source*, Nucl. Instr. and Meth. A **449**, 172 (2000), http://kirkmcd.princeton.edu/examples/detectors/athanassopoluos_nim_a388_149_97.pdf

[8] I. Stancu *et al.*, *The MineBooNE Technical Design Report* (May 14, 2001), http://kirkmcd.princeton.edu/dayabay/MiniBooNE/detector_tdr.pdf

[9] J. Abrhaman *et al.*, *Properties and performance of the prototype instrument for the Pierre Auger Observatory*, Nucl. Instr. and Meth. A **523**, 50 (2004), http://kirkmcd.princeton.edu/examples/detectors/abraham_nim_a523_50_04.pdf

[10] S. Fukuda *et al.*, *The Super-Kamiokande detector*, Nucl. Instr. and Meth. A **501**, 418 (2003), http://kirkmcd.princeton.edu/examples/detectors/fukuda_nim_a501_418_03.pdf

[1]Equation (13) differs slightly from that quoted without derivation in [17], while it agrees with that given by [18].

[11] J. Boger *et al.*, *The Sudbury Neutrino Observatory*, Nucl. Instr. and Meth. A **449**, 172 (2000), http://kirkmcd.princeton.edu/examples/detectors/boger_nim_a449_172_00.pdf

[12] A. Suzuki (for the KamLAND Collaboration), *Present Status of KamLAND*, Nucl. Phys. B (Proc. Suppl.) **77**, 171 (1999), http://kirkmcd.princeton.edu/examples/detectors/suzuki_npbps_77_171_99.pdf

[13] A. Brigatti *et al.*, *The photomultiplier tube testing facility for the Borexino experiment at LNGS*, Nucl. Instr. and Meth. A **537**, 521 (2005), http://kirkmcd.princeton.edu/examples/detectors/brigatti_nim_a537_521_05.pdf

[14] S. Matsuno *et al.*, *Single photon light detector for deep ocean applications*, Nucl. Instr. and Meth. A **276**, 359 (1989), http://kirkmcd.princeton.edu/examples/detectors/matsuno_nim_a276_359_89.pdf

[15] E.G. Anassontzis *et al.*, *The optical module for the NESTOR neutrino telescope*, Nucl. Instr. and Meth. A **479**, 439 (2002), http://kirkmcd.princeton.edu/examples/detectors/anassontzis_nim_a479_439_02.pdf

[16] M. Taiuti, *Wild Ideas on Photon Detection* (Oct. 8,2003), http://www.vlvnt.nl/talks/P5/P5.5-Taiuti.pdf

[17] A. Mager *Magnetic Shields*, IEEE Trans. Magn. **6**, 67 (1970), http://kirkmcd.princeton.edu/examples/detectors/mager_ieeetm_6_67_70.pdf

[18] R. Fitzpatrick, *Magnetic Shielding*, http://farside.ph.utexas.edu/teaching/jk1/lectures/node52.html